



Islamic Azad University
Mashhad Branch

An Algorithm for Modeling and Interpretation of Seismoelectric Data

Ehsan Golmakani Torghabeh^{*1}, Mohammad Ebrahimi Dabbagh², Hooman Latifi¹

¹*Phd student, Science and Research Branch Islamic Azad University, Tehran, Iran*

²*Phd, Islamic Azad University, Shirvan, Iran*

Received 15 July 2012; accepted 20 August 2012

Abstract

Generally speaking, seismoelectric modeling is a prospecting method based on seismic and electromagnetic waves, in which waves generated by a seismic source at the boundary of the two environments generate a relative fluid-solid motion formed as a result of antagonism between the elastic properties of the environment with the saturated fluid. This research has as its objective, a study of the effect of an electric field due to DC current on the propagation of seismic waves by pseudo spectral time domain method, or the more general concept of seismoelectric coupling effect. In this research, poroelastic equations were used for seismic waves and Maxwell's equations for electromagnetic waves. Additionally, the seismoelectric effect or charge density, electrical conductivity, dielectric permittivity function, fluid viscosity and zeta potential were determined. DC electric field variations were compared with results of a physical experiment conducted in a modeled environment. The results revealed that DC electric significantly affected the propagation of elastic energy through seismoelectric coupling in a wide range of seismic frequency widths. Additionally, the boundaries of the substrata were specified using the horizontal component of the electric field of the magnetic wave.

Keywords: *Electric field, Pseudospectral time domain, Poroelastic media, Seismoelectric coupling, Pore pressure.*

1. Introduction

In a porous environment saturated with fluid, mechanical and electromagnetic turbulences couple together. Such coupling is called the electrostatic phenomenon. Seismic waves generate relative fluid-solid motion. Such motion in turn induces electrical current flow. The seismic pulse generates an imbalance in this electrical current flow when passing through an environment, the result of which is measurable as electromagnetic turbulence on the ground's surface. Thompson (1936) proposed that coupling between seismic waves and electric waves can be used as a prospective tool. Some scientist such as Ivanov (1940) reported field measurements of seismoelectric phenomenon in sedimentary material in 1930-1940, and proposed an electrosynthetic mechanism for this conversion. These signals are observed whenever a seismic wave reaches the neighborhood of a bipolar sensor connected to the earth. The time interval between the explosion and the reception of a seismoelectric response depends on the distance between the location of the explosion and the location of the receiver. It does not depend on the distance between the point of the explosion and the interface or intended target. Since Ivanov's report, there have been many other reports of field seismoelectric effects that are related to electrosynthetic phenomenon.

Other scientists such as Martner and Sparks (1959) recorded clearer seismoelectric responses from aerated surfaces. Also, in-well measurements Parkhomenko and Gaskarov (1971) indicated that seismoelectric responses were stronger for limestone than they were for clay. Kepic et al.(1995) found out that piezoelectric responses of a quartz thread were associated with other responses from neighboring sediments and the host rock. Reports of large-scale field experiments by Thompson and Gate (1993) revealed that electro synthetic conversion can be visualized from the boundary of impenetrable rocks and sand saturated with water at a depth of 300 m. Garambois and Dietrichz (2001) showed transient electric fields produced by seismic stimulation. In this essay, first, substratum discoveries are studied by seismoelectric method, and then, the theoretical basis of this method, its procedure, and application are studied. Also, finite difference time domain method is used for reticulation of environment, while pseudospectral time domain method is used for solving spatial derivations, and the algorithm for modeling and interpretation of seismoelectric data is presented. Finally, the application of the model proposed for study of PSTD algorithm is discussed and interpretation of the data resulting from these respective diagrams is presented.

2. Seismoelectric Method

Seismoelectric effects are in principle electro magnetic signals that are generated when seismic

*Corresponding author.

E-mail address (es): golmakani.ehsan@gmail.com

waves cause tension on the earth. Three of these effects are of significant importance (Battler et al, 1996):

a) Electrosynthetic effects induced by seismic waves that are similar to the flow potential. These effects are used to specify the boundary of a shallow substratum in impenetrable formations. The main advantage of this method is the ability to specify thin substrata, which is difficult, or, in some cases, impossible to implement by other geophysical visualization methods. This is because the wave length of the electromagnetic wave that is used to specify boundaries is much smaller than that of the seismic wave. This method can also be used to characterize impenetrable areas.

b) Piezoelectric Effect: This effect is used to visualize and detect quartz threads and pegmatite masses such as gold and other commercial ores.

c) Nonlinear Effects: These effects are produced as instant responses within radio frequency range and high audible frequencies in a sulfide mass. These effects are used to prospect sulfide masses. High resolution of seismic microwave and highly differentiated electroseismic properties of stones give us a perspective of the detailed specifications of mineral masses.

3. Theory of Seismic Wave-Induced Electrosynthetic Effect

When seismic waves propagate in a sedimentary material saturated with fluid, relative solid-fluid motion is induced to a small extent. The force generating such relative motion is a combination of fluid pressure gradients and grain accelerations generated by this wave. Chemically bound surface charges often accumulate on surface grains that are in contact with an electrolyte fluid which reaches a balance with the opposite charges through a scattered distribution of mobile ions in a thin fluid layer around each grain. Opposite ions in this scattered layer are free to move if the fluid moves. Therefore, seismic waves produce flux electric currents that function as a source in Maxwell's equations, and form a basis for the combination of electromagnetic waves with seismic waves (Pride and Haartsen, 1996). Seismic waves produced by mechanical interaction, due to passing through an electrochemical environment, produce a time-varying current, resulting in regional separation of the electrical charges on two sides of the interface. As noted earlier, charge separation happens only when such seismic waves pass through the interface and function as the independent source for propagating electromagnetic waves (Haartsen and Pride, 1997).

4. Equations Governing Seismoelectric Phenomenon

For propagation of seismoelectric waves in porous layered environments saturated with fluid, a wave front modeling technique is presented. This modeling is based on electromagnetic equations and coupled elasticity for a porous fluid-saturated environment (Pride, 1994). Biot and Maxwell's equations along with transfer flux-force equations are used, in which it is hypothesized that propagation of elastic waves in the environment is controlled by Biot's equations for a fluid-saturated porous environment. In the frequency range, we have:

$$1) \nabla \cdot \bar{T} = -\omega^2 [\rho \bar{U} + \rho_f \bar{\omega}]$$

$$2) \bar{T} = [K_G \nabla \cdot \bar{U} + C \nabla \cdot \bar{\omega}] \underline{I} + G [\nabla \bar{U} + \nabla \bar{U}^T - \frac{2}{3} \nabla \cdot \bar{U} \underline{I}]$$

$$3) -p = C \nabla \cdot \bar{U} + M \nabla \cdot \bar{\omega}$$

Where T denotes bulk stress in the environment, P is pressure in porous fluid, U is movement of the solid section, and $\bar{\omega}$ is relative fluid-solid motion. ρ denotes bulk density of the environment and ρ_f is the fluid's density. K_G , G, C and M are Biot's modules and toughness of the environment and I is identity tensor. Electromagnetic effects in the environment are expressed by Maxwell's equations. These equations are presented in grain scale and boundary conditions for fluid and solid phases. Then the weighed average of these equations is found so that the intended macroscopic equations can be obtained. Numerous integrals presented in macroscopic transfer equation required the connection of local fields of fluid flow and electrical flow in the pores' spaces to their respective macroscopic fields. Therefore, questions of boundary value controlling pore scale fields are considered and then the remaining integrals are calculated to obtain macroscopic transfer coefficients. For two-phase porous material (fluid-solid), K_G (Gasman bulk module), C and M, bulk solid and solid modules (K_s , K_f), and module of grains' framework bulk module (K_{fr}) can be expressed as follows:

Input Parameters, Opening Files, Partitioning Memory, Initializing Fields, Calculating Speed V, Calculating Pressure N, Calculating Pressure of Pore P, Calculating Electrical Potential U, Calculating Electrical Field E, Saving Results, Exit

$$4) K_G = \frac{k_{fr} + \phi k_f + (1 + \phi) k_s D}{1 + D}$$

$$5) C = \frac{k_f + k_s F}{1 + D}$$

$$6) M = \frac{1}{\phi} \frac{k_f}{1 + D}$$

Where D is:

$$7) D = \frac{k_f}{\phi k_s^2} [(1 - \phi) k_s - k_{fr}]$$

Where ϕ denotes porosity and G is the shear module of the grain's framework, which can be determined both experimentally and from the theoretical models for the specific pore or the specific geometry of the grain. For convenience sake, we will use toughness H instead of Gasman module, which is defined as follows:

$$8) H = K_G + 4 \frac{G}{3}$$

5. Study of Maxwell's Equations for research on Electromagnetic Field in Static Conditions and Calculation of Electric Field of Reflected Wave

Considering that the frequency of the electromagnetic waves caused by seism is less than 100 Hz, we can consider the conditions to be static and therefore Maxwell's equations can be rewritten as follows:

$$9) \nabla \times E = 0$$

$$10) \nabla \times H = j$$

$$11) \nabla \cdot (\mu H) = 0$$

$$12) \nabla \cdot (\epsilon E) = \rho_e$$

5-1. Mechanism of Seismoelectric Coupling

Due to coupling property, a current is generated in a porous environment due to coupling of the elastic field. As a result, total density of the electrical current is obtained through the summation of density due to electrical field and density as a result of the coupling of the elastic field:

$$13) j = \sigma E + j_s$$

5-2. Study of Seismoelectric in Presence of External Electrical Field

Normally, very weak signals of seismoelectric effect are much harder to recognize than electrostatic signals. This technical problem hinders application of seismoelectric for experimental purposes. A solution to this technical problem is to increase the context electrical field through injecting a direct current in order to generate a temporary context electrical field. If an external electrical field is applied, the density of the final current as noted in relation (22-4) will be summed to a JO that is related to the density of the source of the external current.

$$14) j = \sigma E + j_s + j_0$$

In which case, E includes the source of the external current as well.

5-3. Numerical Algorithm

In order to rewrite the relations calculated in the previous section, and use them as the basis of coding, we will use a numerical algorithm. Using this algorithm, all previous relations will be rewritten as follows:

$$15) \begin{cases} \rho \frac{\partial v_x}{\partial t} = \frac{\partial \sigma_{xx}}{\partial x} + \frac{\partial \sigma_{xy}}{\partial y} - (1-C') \frac{\partial P}{\partial x} + \rho_e E_x + S_x \\ \rho \frac{\partial v_y}{\partial t} = \frac{\partial \sigma_{xy}}{\partial x} + \frac{\partial \sigma_{yy}}{\partial y} - (1-C') \frac{\partial P}{\partial y} + \rho_e E_y + S_y \end{cases}$$

$$16) \begin{cases} \frac{\partial \sigma_{xx}}{\partial t} = (\lambda + 2\mu) \frac{\partial v_x}{\partial x} + \lambda \frac{\partial v_y}{\partial y} \\ \frac{\partial \sigma_{yy}}{\partial t} = (\lambda + 2\mu) \frac{\partial v_y}{\partial y} + \lambda \frac{\partial v_x}{\partial x} \\ \frac{\partial \sigma_{xy}}{\partial t} = \mu \left(\frac{\partial v_x}{\partial y} + \frac{\partial v_y}{\partial x} \right) \end{cases}$$

$$17) \frac{\partial P}{\partial t} = -D \left(\frac{\partial v_x}{\partial x} + \frac{\partial v_y}{\partial y} \right)$$

$$18)$$

$$\frac{\partial}{\partial x} \left(\sigma \frac{\partial U}{\partial x} \right) + \frac{\partial}{\partial y} \left(\sigma \frac{\partial U}{\partial y} \right) = \frac{\epsilon \zeta}{\eta} \left(\frac{\partial^2 P}{\partial x^2} + \frac{\partial^2 P}{\partial y^2} \right) - \left(\frac{\partial j_{0x}}{\partial x} + \frac{\partial j_{0y}}{\partial y} \right)$$

5-4. Solving PSTD for Poroelastic Fields

To properly solve the above equations in a numerical manner, we use Finite-Difference Method. To use this method, first, we have to partition the space of our model into a finite number of cells, each of which are located at point (I, j) and have dimensions of Δx and Δy . All the components of field and features of the environment are calculated at the center of each cell and then we calculate the average of all cells. Spatial derivatives of said equations can be calculated using PSTD method. After applying this method, equations (15)-(18) will be rewritten as follows:

Fig. 2. Layered model for model propagation of seismic wave influenced by DC electric current.

Resulting speed is:

$$19) \begin{cases} v_x^{(n+1)}(i, j) = v_x^{(n)}(i, j) + \frac{\Delta t}{\rho} \left[\bar{D}_x \left(\sigma_{xx}^{(n+\frac{1}{2})}(i, j) \right) + \bar{D}_y \left(\sigma_{xy}^{(n+\frac{1}{2})}(i, j) \right) \right. \\ \quad \left. - (1-C') \bar{D}_x \left(P^{(n+\frac{1}{2})}(i, j) \right) + \rho_e E_x^{(n+\frac{1}{2})}(i, j) + S_x(i, j) \right] \\ v_y^{(n+1)}(i, j) = v_y^{(n)}(i, j) + \frac{\Delta t}{\rho} \left[\bar{D}_x \left(\sigma_{xy}^{(n+\frac{1}{2})}(i, j) \right) + \bar{D}_y \left(\sigma_{yy}^{(n+\frac{1}{2})}(i, j) \right) \right. \\ \quad \left. - (1-C') \bar{D}_y \left(P^{(n+\frac{1}{2})}(i, j) \right) + \rho_e E_y^{(n+\frac{1}{2})}(i, j) + S_y(i, j) \right] \end{cases}$$

Stress is:

$$20) \begin{cases} \sigma_{xx}^{(n+\frac{1}{2})}(i,j) = \sigma_{xx}^{(n-\frac{1}{2})}(i,j) + \Delta t [(\lambda + 2\mu)\bar{D}_x(v_x^{(n)}(i,j)) + \lambda\bar{D}_y(v_y^{(n)}(i,j))] \\ \sigma_{yy}^{(n+\frac{1}{2})}(i,j) = \sigma_{yy}^{(n-\frac{1}{2})}(i,j) + \Delta t [(\lambda + 2\mu)\bar{D}_y(v_y^{(n)}(i,j)) + \lambda\bar{D}_x(v_x^{(n)}(i,j))] \\ \sigma_{xy}^{(n+\frac{1}{2})}(i,j) = \sigma_{xy}^{(n-\frac{1}{2})}(i,j) + \Delta t \mu [\bar{D}_y(v_x^{(n)}(i,j)) + \bar{D}_x(v_y^{(n)}(i,j))] \end{cases}$$

Pressure of pore is:

$$21) P^{(n+\frac{1}{2})}(i,j) = P^{(n-\frac{1}{2})}(i,j) - \Delta t D [\bar{D}_y(v_x^{(n)}(i,j)) + \bar{D}_x(v_y^{(n)}(i,j))]$$

In the above relations, each stage, time difference, Δt , and in calculated in n^{th} time interval, Dx is defined as follows:

$$22) \frac{\partial W(i,j)}{\partial x} = \bar{D}_x(W(i,j)) = F_x^{-1}(ik_x F_x(W(i)))_j$$

To calculate potential U , first, we calculate distance between electrodes and then calculate U using the above relations.

$$23) U = \rho I / 2\pi(1/r_1 - 1/r_2)$$

To obtain electric field resulting from response of interface, first we calculate the potential difference between the two surfaces, and, then, having determined distances Δx , we calculate the electric field.

$$24) E_x^{(n+\frac{1}{2})}(i,j) = -\bar{D}_x \left(U^{(n+\frac{1}{2})}(i,j) \right)$$

$$25) E_y^{(n+\frac{1}{2})}(i,j) = -\bar{D}_y \left(U^{(n+\frac{1}{2})}(i,j) \right)$$

5-5. Numerical Application

In this research, quasispectral time-difference algorithm was used to simulate the poroelastic field while finite difference time domain method was used to solve the electric field. For each time phase, the resulting numerical algorithm is as follows:

1. Calculation of velocity fields by equation (19)
2. Calculation of pressure fields σ by equation (20)
3. Calculation of pressure of pore by equation (21)
4. Solving equations (23) to obtain electrical potential U
5. Calculation of electrical fields E from electrical potential by equations (24) and (25)

Flowchart of program shows the process in more detail in Fig. 1.

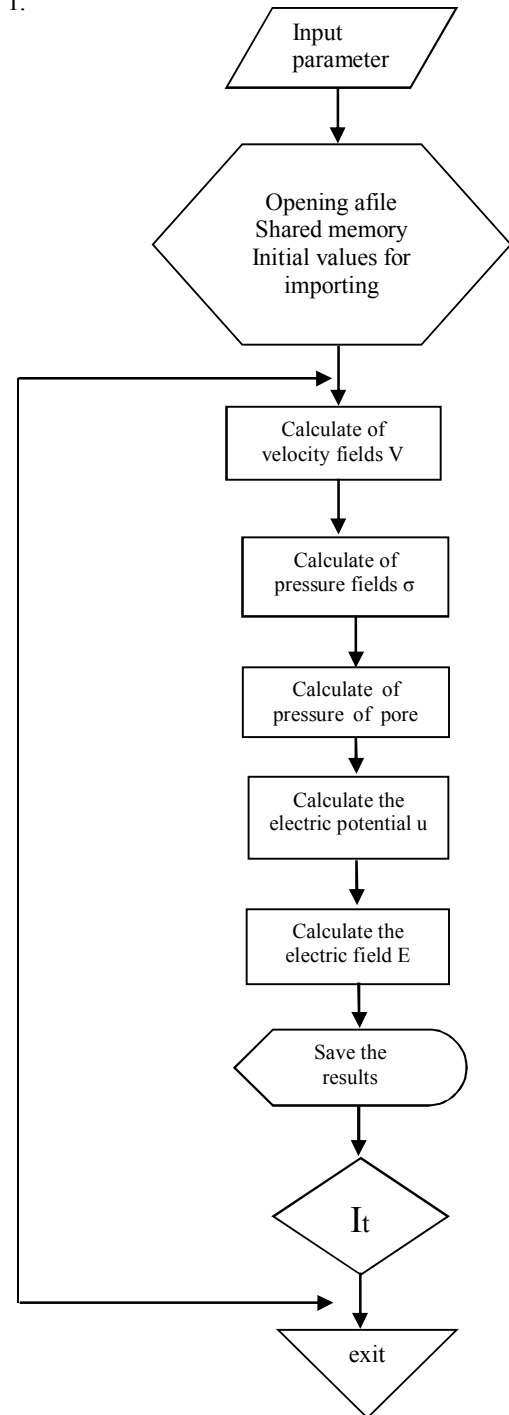


Fig. 1. Algorithm proposed for modeling and interpretation of seismoelectric data

6. Modeling for Presented Algorithm and Processing and Interpretation of Obtained Data

Using the obtained algorithm, we can simulate the propagation of an elastic wave in a poroelastic environment influenced by a DC electrical field. Here, a three-layer model (table 1) is used for modeling

propagation of a seismic wave influenced by DC electric current.

Table 1. Parameters used in modeling, V_p denotes velocity of wave p in layer, ρ is special resistance in each layer, z is depth of each layer

Specifications of layer	$V_p(m/s)$	$(\Omega m) \rho$	Z(m)
First layer	2350	20	250
Second layer	2580	100	500
Third layer	2580	200	850

The above model is 3.2 km wide and 1.6 km deep. Electrodes are spaced at 2000 m distances in the intended model. An Elastic source is used and receivers are placed between two electrodes. The used source is spaced out from the positive electrode. The signal frequency of the elastic source of the pulse wave is Hz. Sixty receivers with 25 cm spatial spacing are placed on the right side. The time interval used is 1/1000 second, and the overall time stages are 15,000. DC current ranging from 0 to 25 A is injected from electrode 2 to the model at 100 time phases. The source explodes at an isotropic pressure of 1,000 P at 50 m away from the positive electrode at 0.2 s.

Using the presented model shown in figure 2, all relations related to the proposed algorithm are calculated through programming and the results are shown in the form of a diagram.

Figure 3 shows variations in velocity in the second and third layers. It is seen that as the distance between receiver and positive electrode changes, the velocity of the wave incident on the interface of the layers varies at different times, and because distances are increasing, the velocity of the wave also gradually increases.

In figure 4, we study variations in the electrical field at the boundary of two layers (second and third). Considering the above relation, horizontal electrical field $E_x = -D_x U$, first, we calculate the potential at the boundary of the two layers for different electrode spacing, and then, from the said relation, we calculate the horizontal electrical field in terms of variations in distance, and draw its diagram. It is seen that the electrical field decreases as the distance increases.

By superimposing figures 3 and 4, we obtain figure 5, which is a time versus distance diagram, and which well represents variations in the electrical field induced between the two layers. This diagram represents the response of the interface of the two layers, which in its own right is one of the important sources of production of induced electrical signals.

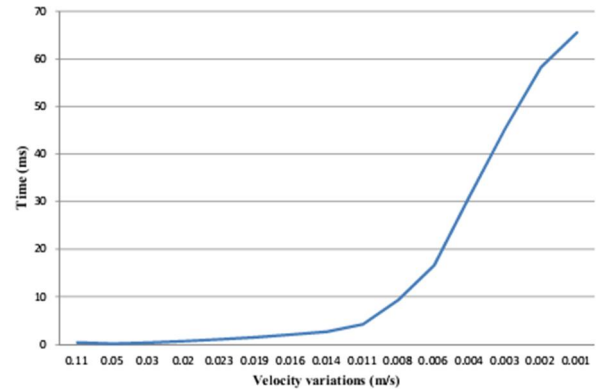


Fig. 3. Velocity variations versus time in-between second and third layers.

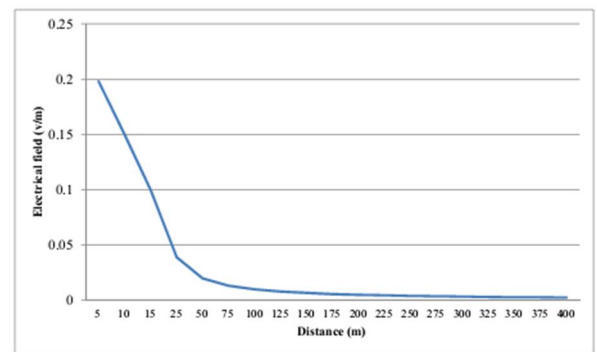


Fig. 4. Variations in electrical field in X direction in terms of distance.

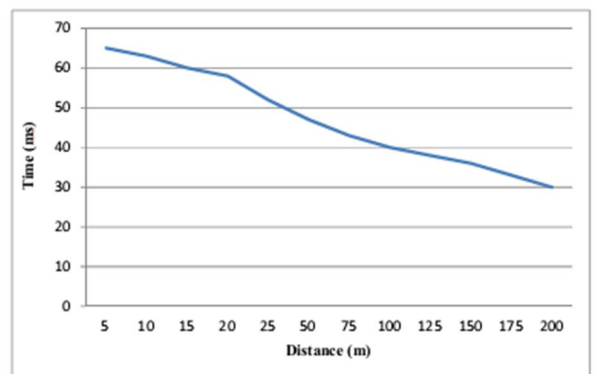


Fig. 5. Variations in electrical field at interface of second and third layers.

6. Conclusion

The seismoelectric method was previously used in the study of heterogeneous alluvial formation of two layers in northern Tehran, where modeling of the data was conducted based on reflection matrix, generalized transition matrix and inverse conversion matrix methods in the field of time-space. Processing of the resulting data was conducted using sinusoidal deduction method. The method presented in this article

is a study of seismoelectric method for a structure with more than two layers. It is expressed using finite difference methods for differential equations and calculation of the produced electrical field. Pseudospectral time difference method was used for the calculation of variable derivatives in the field of Fourier, which requires at least two nodes in each wavelength in order to produce accurate solutions. After calculating these relations and studying the seismoelectric phenomenon in the presence of an external electrical field, the algorithm in question was proposed, and a real three-layer model was modeled based on this algorithm. The results thereof were presented in the form of a diagram. The results of this research are briefly as follows:

Modeling of the response of the interface of layers (especially hydrated layers) in its own right, functions as an important source of induced electrical signals.

Using the proposed model, we can easily see the response of the interface as induced electrical signals.

In this research, a series of equations including equations of velocity, stress, pressure of pore, electrical potential and electrical field for seismoelectric connection in poroelastic environment were calculated for the purpose of simulating the propagation of elastic waves in a porous environment influenced by DC electrical field. It became clear that in a frequency band of seismic waves, electromagnetic fields with a constant electrical field can be estimated.

Numerical simulation of propagation of an elastic wave in a poroelastic environment with DC electrical fields successfully revealed that DC electrical field significantly affects the propagation of seismic waves.

Also, it became clear that the central frequency of seismoelectric waves (110-120 Hz) is higher than the seismic data (30-40 Hz) (because the wavelength of electromagnetic waves is higher than that of mechanical waves)

Acknowledgments

I should like to thank Dr. Mohammad Ali Riahi for his help and recommendations during the course of my work. I would also like to express my gratitude to the respectful referees whose invaluable recommendations improved this article.

References

- Biot, M. A., 1956, Theory of propagation of elastic waves in a fluid-saturated porous solid: *J. Acoust. Soc. Am.*, 28, 168–191.
- Biot, M. A., 1962a, Mechanics of deformation and acoustic propagation in porous media: *J. Appl. Phys.*, 33, 1482–1498.
- Biot, M. A., 1962b, Generalized theory of acoustic propagation in porous dissipative media: *J. Acoust. Soc. Am.*, 34, 1254–1264.
- Garambois, S., and Dietrichz, M., 2001, Seismoelectric wave conversions in porous media: Field measurements and transfer function analysis: *Geophysics*, 66,(5),1417–1430.
- Haartsen, M. W., and Pride, S., 1997, Electro seismic waves from point sources in layered media: *J. Geophys. Res.*, 102, 24745–24769.
- Haartsen, M. W., and Pride, S. R., 1997, Electro seismic waves from point sources in layered media: *J. Geophys. Res.*, 102, (B11), 24745–24769.
- Ivanov, A. G., 1940, The electro seismic effect of the second kind: *SSR, Ser. Geogr. Geofiz.*, 5, 699–7
- Kepic, A. W., Maxwell, M., and Russell, R. D., 1995, Field trials of a seismoelectric method for detecting massive sulfides: *Geophysics*, 60, (2); 365–373.
- Martner, S. T., and Sparks, N. R., 1959, The electro seismic effect: *Geophysics.*, 24,297–308
- Pride, S., 1994, Governing equations for the coupled electromagnetic and acoustics of porous media: *Phys. Rev. B*50., 15678–15696.
- Pride, S. R., and Haartsen, M. W., 1996, Electro seismic wave properties: *J. Acoust. Soc. Am.*, 100, 1301–1315.
- Parkhonenko, E. A., and Gaskarov, I. V., 1971, Borehole and laboratory studies of the seismoelectric effect of the second kind in rocks: *Izv Akad Nauk SSSR, Physics of the Solid Earth*, 9, 88–92.
- Thompson, A., and Gist, G., 1993, Geophysical applications of electrokinetic conversion: *The Leading Edge.*, 12, 1169–1173.
- Thompson, R., 1936, The seismic-electric effect: *Geophysics*, 1, 327–335.